Inorg. Chem. **2008**, *47*, 5919−5929

Mononuclear Manganese(III) Complexes as Building Blocks for the Design of Trinuclear Manganese Clusters: Study of the Ligand Influence on the Magnetic Properties of the $[Mn_3(\mu_3\text{-}O)]^{7+}$ Core

Marta Viciano-Chumillas,[†,‡] Stefania Tanase,[†] Ilpo Mutikainen,[§] Urho Turpeinen,[§] L. Jos de Jongh,*[,‡] and Jan Reedijk*[,†]

Gorlaeus Laboratories, Leiden Institute of Chemistry, Leiden University, PO Box 9502, 2300 RA Leiden, The Netherlands, Kamerlingh Onnes Laboratory, Leiden Institute of Physics, Leiden University, PO Box 9504, 2300 RA Leiden, The Netherlands, and Laboratory of Inorganic Chemistry, Department of Chemistry, University of Helsinki, P.O. Box 55 (A.I.Virtasen aukio 1), 00014 Helsinki, Finland

Received February 7, 2008

The synthesis, crystal structure, and magnetic properties of three new manganese(III) clusters are reported, $[Mn_3(\mu_3\text{-}O)(phpzH)_3(MeOH)_3(OAc)]$ **(1)**, $[Mn_3(\mu_3\text{-}O)(phpzMe)_3(MeOH)_3(OAc)]\cdot 1.5MeOH$ **(2)**, and $[Mn_3(\mu_3\text{-}O)(phpzH)_3(MeOH)_4(N_3)]\cdot MeOH$ **(3)** (H_2phpzH = 3(5)-(2-hydroxyphenyl)-pyrazole and $H_2phpzMe$ = 3(5)-(2-hydroxyphenyl)-5(3)-methylpyrazole). Complexes **1**−**3** consist of a triangle of manganese(III) ions with an oxido-center bridge and three ligands, $phpzR^{2-}$ (R = H, Me) that form a plane with the metal ions. All the complexes contain the same core with the general formula $[Mn_3(\mu_3\text{-}O)(phpzR)_3]^{+}$. Methanol molecules and additional bridging ligands, that is, acetate (complexes **1** and **2**) and azide (complex **3**), are at the terminal positions. Temperature dependent magnetic susceptibility studies indicate the presence of predominant antiferromagnetic intramolecular interactions between manganese(III) ions in **1** and **3**, while both antiferromagnetic and ferromagnetic intramolecular interactions are operative in **2**.

Introduction

Polynuclear manganese complexes have been extensively studied for two main reasons. The first one is their biological importance as models for the water oxidation center of Photosystem II.[1] The second one is the paramagnetic nature of the manganese ion in various oxidation states providing interesting magnetic properties.[2–4] Thus, a new field entitled *molecular magnetism* has been developed.

Synthetically, numerous efforts have been made to obtain a variety of manganese clusters.[2,5] Two well-known approaches have been developed in the literature. The first one, the designed synthesis of such clusters, is based upon the use of rigid ligands that allow the control of the geometry of the cluster.[6] The second approach is based on the serendipitous assembly of flexible ligands with metal ions, where the use of different synthetic conditions can give rise to a rich chemistry.[7] While carboxylate ligands have been the most studied,[8] considerable efforts have recently been applied to the design of various pyrazole-based ligands showing an interesting coordination chemistry.[9–13]

In this respect, new families of related compounds are very useful for the purpose of controlling the synthesis and investigating the structure/property relationships. To achieve this goal, we have synthesized a family of mononuclear manganese(III) compounds with general

* To whom correspondence should be addressed. E-mail: jongh@physics.leidenuniv.nl (L.J.d.J.), reedijk@chem.leidenuniv.nl (J.R.). Tel.: +31-71-5275466 (L.J.d.J.), +31-71-5274459 (J.R.). Fax: +31-71-5275404 (L.J.d.J.), +31-71-5274671 (J.R.).
† Leiden Institute of Chemistry, Leiden University.
‡ Leiden Institute of Physics, Leiden University.
§ University of Helsinki.

(1) Mukhopadhyay, S.; Mandal, S. K.; Bhaduri, S.; Armstrong, W. H. *Chem. Rev.* **2004**, *104*, 3981–4026.
(2) Aromi, G.; Brechin, E. K. *Struct. Bonding* **2006**, *122*, 1–67.
(3) Christou, G.; Gatteschi, D.; Hendrickson, D. N.; Sessoli, R. *MRS Bull.* **2000**, *25*, 66–71.
(4) Gatteschi, D.; Sessoli, R. *Angew. Chem., Int. Ed.* **2003**, *42*, 268–297.
(5) Christou, G. *Polyhedron* **2005**, *24*, 2065–2075.
(6) Rebilly, J. N.; Mallah, T. *Struct. Bonding* **2006**, *122*, 103–131.
(7) Winpenny, R. E. P. *J. Chem. Soc., Dalton Trans.* **2002**, 1–10.
(8) Aromi, G.; Aubin, S. M. J.; Bolcar, M. A.; Christou, G.; Eppley, H. J.; Folting, K.; Hendrickson, D. N.; Huffman, J. C.; Squire, R. C.; Tsai, H. L.; Wang, S.; Wemple, M. W. *Polyhedron* **1998**, *17*, 3005–3020.

10.1021/ic8002492 CCC: $40.75
Published on Web 06/11/2008

Scheme 1. Phenol-Pyrazole Based Ligands

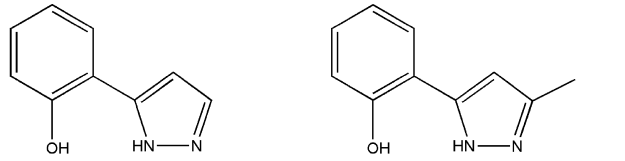

HphpzH
3(5)-(2-hydroxyphenyl)-pyrazole

HphpzMe
3(5)-(2-hydroxyphenyl)-5(3)-methylpyrazole

formula $[Mn(HphpzR)_2X]$, where HphpzR is 3(5)-(2-hydroxyphenyl)-pyrazole (R = H) and 3(5)-(2-hydroxyphenyl)-5(3)-methylpyrazole (R = Me) (Scheme 1) and $X^- = Cl$, Br.[14] In this paper it is shown that these complexes are indeed promising building blocks to synthesize complexes of higher nuclearity containing the core $[Mn_3(\mu_3\text{-}O)(phpzR)_3]^+$ (R = H, Me). The synthesis, X-ray crystal structures, and magnetic properties of the complexes $[Mn_3(\mu_3\text{-}O)(phpzH)_3(MeOH)_3(OAc)]$ **(1)**, $[Mn_3(\mu_3\text{-}O)(phpzMe)_3(MeOH)_3(OAc)]\cdot 1.5MeOH$ **(2)**, and $[Mn_3(\mu_3\text{-}O)(phpzH)_3(MeOH)_4(N_3)]\cdot MeOH$ **(3)** are described here in detail.

Experimental Section

Syntheses. All manipulations were performed using commercial materials as received. The complexes $[Mn(HphpzR)_2X]$ (R = H, Me and X^- = Br, Cl) have been synthesized according to the literature procedure.[14]

Caution! *Azide salts and perchlorate salts are potentially explosive. Such compounds should be used in small quantities and should be treated with utmost care at all times.*

$[Mn_3(\mu_3\text{-}O)(phpzH)_3(MeOH)_3(OAc)]$ (1). $[Mn(HphpzH)_2Br]$ (20 mg, 0.044 mmol) was dissolved in methanol, followed by the addition of a solution of sodium methoxide (7 mg, 0.13 mmol) and a solution of $Mn(OAc)_2\cdot 4H_2O$ (22 mg, 0.089 mmol) in methanol. Green single crystals (18 mg, 0.022 mmol) were obtained by slow evaporation of the reaction mixture in 75% yield. Anal. Calcd for **1** ($C_{32}H_{33}Mn_3N_6O_9$): C, 47.42; H, 4.10; N, 10.37. Found: C, 47.42; H, 4.37; N, 10.65. IR (cm^{-1}): 1599(m), 1541(m), 1515(w), 1481(vs), 1454(m), 1430(m), 1351(w), 1336(m), 1296(vs), 1250(s), 1142(s), 1132(s), 1078(s), 1028(m), 1014(s), 985(m), 860(s), 775(s), 749(vs), 674(vs), 645(vs), 600(vs), 577(m), 449(s), 394(s), 324(s). ESI-MS (*m*/*z*, %): 737 (100) $[Mn_3(\mu_3\text{-}O)(phpzH)_3(MeCN)_2]^+$, 696 (77) $[Mn_3(\mu_3\text{-}O)(phpzH)_3(MeCN)]^+$, 655 (16) $[Mn_3(\mu_3\text{-}O)(phpzH)_3]^+$.

$[Mn_3(\mu_3\text{-}O)(phpzMe)_3(MeOH)_3(OAc)]\cdot 1.5MeOH$ (2). A solution of sodium methoxide (8 mg, 0.14 mmol) in methanol was added to a methanolic solution of $[Mn(HphpzMe)_2Br]$ (21 mg, 0.044 mmol), followed by a solution of $Mn(OAc)_2\cdot 4H_2O$ (22 mg, 0.090 mmol) in methanol. The slow evaporation of the reaction mixture affords green single crystals (16 mg, 0.018 mmol) in 61% yield. Anal. Calcd for **2** ($C_{35}H_{39}Mn_3N_6O_9$, $1.5(CH_4O)$): C, 48.68; H, 5.04; N, 9.33. Found: C, 48.44; H, 4.16; N, 10.67. IR (cm^{-1}): 1599(m), 1558(m), 1532(m), 1496(m), 1456(s), 1405(m), 1297(vs), 1269(s), 1246(s), 1126(s), 1090(w), 1060(m), 1037(m), 864(s), 792(m), 748(vs), 725(vs), 668(vs), 648(vs), 604(vs), 580(s), 418(s), 412(s), 384(vs), 318(s). ESI-MS (*m*/*z*, %): 442 (100) $[Mn(HphpzMe)_2(MeCN)]^+$, 871 (34) $[Mn_3(\mu_3\text{-}O)(phpzMe)_2(HphpzMe)(OAc)(MeOH)_3(H_2O)]^+$, 738 (22) $[Mn_3(\mu_3\text{-}O)(phpzMe)_3(MeCN)]^+$.

$[Mn_3(\mu_3\text{-}O)(phpzH)_3(MeOH)_4(N_3)]\cdot MeOH$ (3). A solution of NaN_3 (17 mg, 0.26 mmol) was added to a solution of $[Mn(HphpzH)_2Cl]$ (30 mg, 0.074 mmol) in MeOH. The solution was stirred for 5 min and filtered, and the green filtrate left undisturbed to concentrate slowly by evaporation. Green crystals appeared within a few weeks in 70% yield. Anal. Calcd for **3** ($C_{32}H_{38}Mn_3N_9O_9$): C, 44.82; H, 4.47; N, 14.70. Found: C, 43.81; H, 3.84; N, 16.30. The discrepancy between calculated and obtained elemental percentages for complex **3** arises from analytical variations because of the incomplete combustion of the sample (the purity of the sample was proven by X-ray crystallography). IR (cm^{-1}): 3352(w), 2039(s), 1599(m), 1563(m), 1512(w), 1481(s), 1454(m), 1429(m), 1352(m), 1338(m), 1297(s), 1250(s), 1144(s), 1130(s), 1078(s), 1036(w), 1007(m), 986(m), 860(s), 782(m), 747(vs), 673(vs), 644(s), 598(vs), 448(s), 390(s), 353(w), 329(w). ESI-MS (*m*/*z*, %): 655(29) $[Mn_3(\mu_3\text{-}O)(phpzH)_3]^+$, 696(72) $[Mn_3(\mu_3\text{-}O)(phpzH)_3(MeCN)]^+$, 736(100) $[Mn_3(\mu_3\text{-}O)(phpzH)_3](MeCN)_2]^+$.

Physical Measurements. Elemental analyses for C, H, and N were performed on a Perkin-Elmer 2400 series II analyzer. Infrared spectra (4000−300 cm^{-1}) were recorded on a Perkin-Elmer Paragon 1000 FTIR spectrometer equipped with a Golden Gate ATR device using the reflectance technique. Electrospray mass spectra (ESI-MS) in acetonitrile solution were obtained on a Thermo Finnigan AQA apparatus. Direct current (DC) magnetic data were recorded using a Quantum Design MPMS-5 SQUID susceptometer. The magnetic susceptibilities were measured from 1.8 to 300 K on polycrystalline samples in a gelatin capsule with an applied field of 0.1 T. The magnetization was measured at 2, 4, and 6 K in the 0−5 T range. Data were corrected for magnetization of the sample holder and for diamagnetic contributions, which were estimated from Pascal constants.[15]

X-ray Crystallography. Intensity data for single crystals of **1**, **2**, and **3** were collected using Mo Kα radiation (λ = 0.71073 Å) on a Nonius Kappa CCD diffractometer. Crystal and refinement data for **2** and **3** are collected in Table 1. The intensity data were corrected for Lorentz and polarization effects and for absorption (multiscan absorption correction).[16] The structures were solved by Patterson methods.[17] The programs EvalCCD,[18] DIRDIF96,[19] SHELXS-97,[20] and SHELXL-97[2122] were used for data reduction,

(9) Tanase, S.; Bouwman, E.; Long, G. J.; Shahin, A. M.; Mills, A. M.; Spek, A. L.; Reedijk, J. *Eur. J. Inorg. Chem.* **2004**, 4572–4578.
(10) Tanase, S.; Aromi, G.; Bouwman, E.; Kooijman, H.; Spek, A. L.; Reedijk, J. *Chem. Commun.* **2005**, 3147–3149.
(11) Tao, J.; Zhang, Y. Z.; Bai, Y. L.; Sato, O. *Inorg. Chem.* **2006**, *45*, 4877–4879.
(12) Bai, Y. L.; Tao, J.; Wernsdorfer, W.; Sato, O.; Huang, R. B.; Zheng, L. S. *J. Am. Chem. Soc.* **2006**, *128*, 16428–16429.
(13) Viciano-Chumillas, M.; Tanase, S.; Aromi, G.; Smits, J. M. M.; de Gelder, R.; Solans, X.; Bouwman, E.; Reedijk, J. *Eur. J. Inorg. Chem.* **2007**, 2635–2640.
(14) Viciano-Chumillas, M.; Marqués-Giménez, M.; Tanase, S.; Evangelisti, M.; Mutikainen, I.; Turpeinen, M.; Smits, J. M. M.; de Gelder, R.; de Jongh, L. J.; Reedijk, J., unpublished work.
(15) Kahn, O. *Molecular Magnetism*; Wiley-VCH: New York, 1993.
(16) Sheldrick, G. M. *Program for Empirical Absorption Correction*; University of Göttingen: Göttingen, Germany, 1996.
(17) Beurskens, P. T.; Beurskens, G.; Strumpel, M.; Nordman, C. E. In *Patterson and Pattersons*; Clarendon Press: Oxford, 1987; p 356.
(18) Duisenberg, A. J. M.; Kroon-Batenburg, L. M. J.; Schreurs, A. M. M. *J. Appl. Crystallogr.* **2003**, 220.
(19) Beurskens, P. T.; Beurskens, G.; Bosman, W. P.; De Gelder, R.; Garcı´a-Granda, S.; Gould, R. O.; Israël, R.; Smits, J. M. M.; Smykalla, C. *The DIRDIF96. A computer program system for the crystal structure determination by Patterson methods and direct methods applied to difference structure factors*; Crystallography Laboratory, University of Nijmegen: Nijmegen, The Netherlands, 1996.
(20) Sheldrick, G. M. *SHELXS-97: Program for Crystal Structures Determination*; University of Göttingen; Germany: Göttingen, 1997.
(21) Sheldrick, G. M. *SHELXL-97: Program for Crystal Structure Refinement*; University of Göttingen: Göttingen, Germany, 1997.
(22) Duisenberg, A. J. M. Reflections on area detectors. Utrecht, 1998.

Table 1. Crystal Data and Structure Refinements for $[Mn_3(\mu_3\text{-}O)(phpzMe)_3(MeOH)_3(OAc)]\cdot 1.5MeOH$ **(2)** and $[Mn_3(\mu_3\text{-}O)(phpzH)_3(MeOH)_4(N_3)]\cdot MeOH$ **(3)**

	formula	
	$C_{35}H_{39}Mn_3N_6O_9$, 1.5(CH_4O) **(2)**	$C_{32}H_{38}Mn_3N_9O_9$ **(3)**
formula mass [g mol^{-1}]	900.61	857.53
crystal system	monoclinic	monoclinic
space group	*C*2/*c*	*C*2/*c*
a [Å]	25.535(5)	45.999(9)
b [Å]	8.038(2)	7.512(2)
c [Å]	39.853(9)	23.563(5)
α [°]	90	90
β [°]	95.51(3)	116.35(3)
γ [°]	90	90
V [Å^3]	8142(3)	7296(3)
Z	8	8
D_{calc} [g cm^{-3}]	1.469	1.561
crystal size	0.02 × 0.11 × 0.30	0.18 × 0.20 × 0.22
crystal shape and color	needles and green	blocks and green
number of collected reflections (unique)	39218(6877)	24373(6288)
number of observed reflections ($I_o > 2\sigma(I_o)$)	2862	4420
internal *R* factor	0.185	0.043
number of parameters	513	482
goodness-of-fit *S* on F^2	1.04	1.04
μ [mm^{-1}]	0.979	1.088
$R_1{}^a$ [$I > 2.0\sigma(I)$]	0.0976	0.0381
$wR_2{}^b$ [all data]	0.2456	0.0901
T [°C]	173	173

^{a} $R_1 = \Sigma||F_o| - |F_c||/\Sigma|F_o|$. ^{b} $wR_2 = \{\Sigma[w(F_o^2 - F_c^2)^2]/\Sigma w(F_o^2)^2\}^{1/2}$.

structure solution, and refinement, respectively. All non-hydrogen atoms were refined with anisotropic displacement parameters. All hydrogens were placed at calculated positions and were refined riding on the parent atoms. CCDC-674691 **(1)**, 674692 **(2)**, and 674693 **(3)** contain the supplementary crystallographic data for this paper. These data can be obtained free of charge at www.ccdc.cam.ac.uk/conts/retrieving.html [or from the Cambridge Crystallographic Data Centre, 12, Union Road, Cambridge CB2 1EZ, U.K.; fax: (internat.) +44−1223/336−033; E-mail: deposit@ccdc.cam.ac.uk]. Geometric calculations and molecular graphics were performed with the PLATON package.[23]

Results and Discussion

Syntheses. Mononuclear complexes with the general formula $[Mn(HphpzR)_2X]$ (R = H, Me; X^- = Br, Cl)[14] prove to be excellent starting materials for high-nuclearity manganese(III) complexes as it is shown in the present work. Complexes **1** and **2** were synthesized with the addition of manganese(II) acetate to $[Mn(HphpzR)_2Br]$ (R = H, Me) in the presence of sodium methoxide. An alternative route was reported very recently by others[11] for complex **1**, using only the manganese(II) acetate salt. Following the same published procedure, with the ligand 3(5)-(2-hydroxyphenyl)-5(3)-methylpyrazole, H_2phpzMe, we have found that complex **2** can also be obtained in 82% yield. Additionally, both complexes can be synthesized using the reaction of the manganese(II) acetate salt with the ligand H_2phpzR (R = H, Me) in the presence of NaO_2CMe and NaOMe. The presence of the acetate at the axial position in both complexes **1** and **2** has led us to try other carboxylates as well. This work is under current investigation and will be published in subsequent papers.

(23) Spek, A. L. *PLATON, A Multipurpose Crystallographic Tool*; Utrecht University: The Netherlands, 2003.

Complex **3** was obtained by reaction of $[Mn(HphpzH)_2Cl]$ and NaN_3 in methanol. The same complex can also be synthesized from manganese(II) chloride in the presence of H_2phpzH, sodium azide, and triethylamine in methanol. The infrared spectrum reveals the presence of the azide exhibiting a sharp band at 2039 cm^{-1}. Following the synthetic procedures of complex **3**, with the ligand H_2phpzMe, small crystals were obtained. Better quality is needed to report them. Scheme 2 summarizes the synthetic procedures and complexes obtained that are presented in this paper.

The ESI-MS studies for complexes **1**−**3** clearly show the stability of the core $[Mn_3(\mu_3\text{-}O)(phpzR)_3]^+$ (R = H, Me) in solution. Therefore, the possibility of using them as building blocks for the synthesis of even higher nuclearity complexes is currently under investigation.

Description of the Crystal and Molecular Structures. The X-ray structure of complex **1** has been reported independently by others during the progress of this work.[11] It consists of an equilateral triangle formed by three manganese(III) ions that are bridged by a central oxygen. The deprotonated ligands $phpzH^{2-}$ are in a plane with their manganese(III) ions. Three methanol molecules and an acetate group are at the apical positions. As a result, all the three manganese(III) ions are hexacoordinated. The trinuclear units are linked by an acetate bridge. The Mn···Mn distances in the trinuclear unit are 3.306 Å, 3.313 Å, and 3.307 Å for Mn(1)···Mn(2), Mn(1)···Mn(3), and Mn(2)···Mn(3), respectively. The μ_3-O^{2-}(O1) ion is 0.110 Å above the Mn_3 plane. The Mn−O(1) distances are 1.917(2) Å for Mn(1), 1.904(2) Å for Mn(2), and 1.919(2) Å for Mn(3). The Mn−O(1)−Mn angles are Mn(1)−O(1)−Mn(2) = 119.78(12)°; Mn(1)−O(1)−Mn(3) = 119.47(11)°, and Mn(2)−O(1)−Mn(3) = 119.77(11)°.

Complex **2** crystallizes in the monoclinic space group *C*2/*c*. The crystal structure is shown in Figure 1. The structure analysis reveals a trinuclear manganese(III) complex containing a μ_3-oxido bridge. Each edge of the Mn_3 triangle is bridged by a $\eta^1/\eta^1/\mu$-pyrazolato ligand with the phenolic oxygen and one pyrazole nitrogen atom chelating a Mn(III) ion. Selected bond lengths and angles are listed in Table 2. Intracluster Mn···Mn distances are 3.338 Å, 3.269 Å, and 3.227 Å for Mn(1)···Mn(2), Mn(1)···Mn(3), and Mn(2)···Mn(3), respectively. The μ_3-O^{2-}(O1) ion is 0.171 Å above the Mn_3 plane. The Mn−O(1) distances are 1.900(6) Å for Mn(1), 1.943(6) Å for Mn(2), and 1.859(7) Å for Mn(3). The Mn−O(1)−Mn angles are Mn(1)−O(1)−Mn(2) = 120.6(4)°; Mn(1)−O(1)−Mn(3) = 120.9(3)°, and Mn(2)−O(1)−Mn(3) = 116.1(3)°. Mn(1) and Mn(2) are hexacoordinated; Mn(1) contains two methanol molecules at the axial positions, while Mn(2) is axially coordinated to a methanol molecule and an acetate ion. Mn(3) is pentacoordinated with an acetate ion at the axial position. The main difference with complex **1** is that in this case the acetate is bridging two manganese(III) ions from the same trinuclear unit, whereas in complex **1** it is binding two manganese(III) ions from different trinuclear units. Consequently, in complex **1** a chain is formed. Probably this difference arises from the steric hindrance of the methyl group from the pyrazole ring of the ligand. In

Scheme 2. Synthetic Procedures of Manganese(III) Complexes

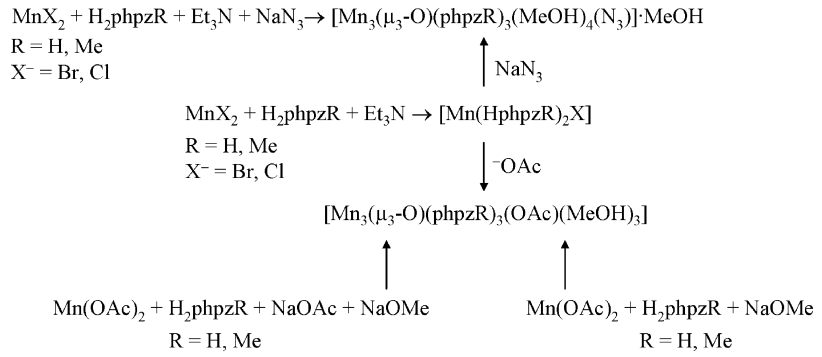

complex **2**, one and a half-solvent molecules are present in the unit cell. Intramolecular hydrogen bonds are observed between the acetate group and coordinated methanol and the solvent present in the unit cell (Supporting Information, Table S1 and Figure S1).

Complex **3** crystallizes in the monoclinic space group *C*2/*c*. As shown in Figure 2, **3** consists of a trinuclear manganese(III) core in which the Mn(III) ions are bridged by a central oxido. These trinuclear units are bridged by a single azide ion in an end-to-end binding mode. The three deprotonated H_2phpzH ligands form a plane with the manganese(III) ions. The μ_3-O^{2-}(O1) ion lies 0.040 Å above the Mn_3 triangle. The metal ions are all hexacoordinated. Mn(1) and Mn(2) contain a methanol molecule and an azide molecule at the axial positions while in Mn(3) two methanol molecules occupy the axial positions. Selected bond lengths and angles are listed in Table 3. The Mn−O(1) average distance is 1.913 Å. The Mn···Mn distances in the trinuclear unit are 3.329 Å, 3.326 Å, and 3.299 Å for Mn(1)···Mn(2), Mn(1)···Mn(3), and Mn(2)···Mn(3), respectively. The Mn−O(1)−Mn angles are Mn(1)−O(1)−Mn(2) = 120.79(12)°, Mn(1)−O(1)−Mn(3) = 120.11(14)°, and Mn(2)−O(1)−Mn(3) = 118.96(12)°. The Mn−N_{azido} distances are 2.327(3) Å and 2.339(4) Å. The shortest Mn···Mn distance between the trinuclear units is 6.483 Å through the azide bridge, which is slightly longer than the acetate-bridged distance in **1** (6.418 Å). The shortest interchain Mn···Mn distance is 8.153 Å between the Mn(1). A methanol molecule in the lattice forms hydrogen bonds with a coordinated methanol (O(2)−H(2A)···O(10) 2.709(4) Å) and the phenoxido moiety of a $phpzH^{2-}$ bridging ligand (O(10)−H(10D)···O(121) 2.932(4) Å) (Supporting Information, Table S1 and Figure S2).

Magnetic Properties. Magnetic susceptibilities were measured under a 0.1 T field in the 1.8−300 K temperature range for the complexes **1**−**3**. The temperature dependence of the $\chi_M T$ product for complex **1** is shown in Supporting Information, Figure S3; the magnetic behavior observed is identical to that reported earlier.[11]

As shown in Figure 3, the $\chi_M T$ value of **2** is 9.14 cm^3 K mol^{-1} at 300 K, which is slightly above the limiting spin-only value (9.0 cm^3 K mol^{-1}) calculated for three *noninteracting* manganese(III) ions, assuming an isotropic *g*-value of 2.00.[15] When lowering the temperature, the $\chi_M T$ product decreases gradually to 2.90 cm^3 K mol^{-1} at 15 K, and then more rapidly to 1.97 cm^3 K mol^{-1} at 1.8 K. For complex **3**, the $\chi_M T$ value is 8.80 cm^3 K mol^{-1} at 300 K, slightly lower than the noninteracting spin-only limit. As shown in Figure 4, the $\chi_M T$ product shows a similar decrease with temperature as for **2**, reaching an even lower value of 0.74 cm^3 K mol^{-1} at 1.8 K. The observed behavior suggests the presence of

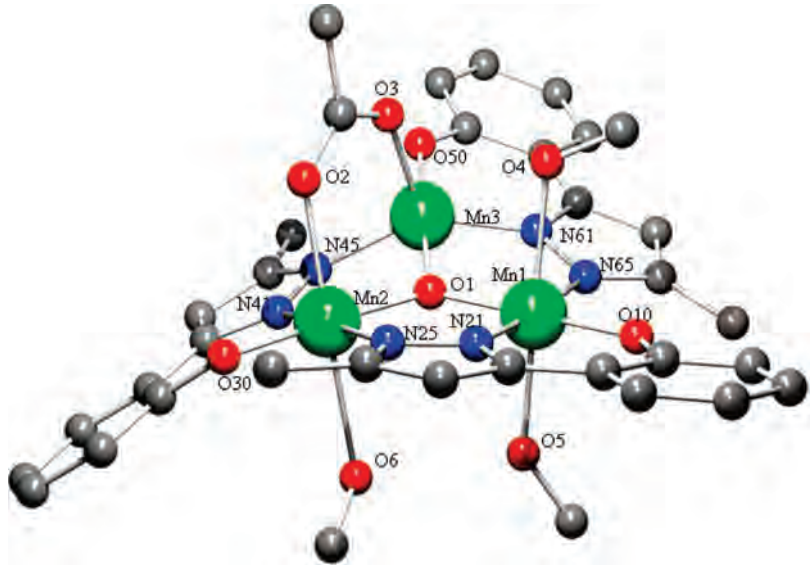

Figure 1. Pluton projection of the complex [Mn_3(μ_3-O)(phpzMe)$_3$(MeOH)$_3$(OAc)] (**2**). Noncoordinated methanol molecules and hydrogen atoms have been omitted for clarity.

Table 2. Selected Bonds Lengths [Å] and Angles [°] for the Complex $[Mn_3(\mu_3\text{-}O)(phpzMe)_3(MeOH)_3(OAc)]\cdot 1.5MeOH$ (**2**)

Bond Lengths			
Mn(1)−O(1)	1.900(6)	Mn(1)−O(4)	2.366(8)
Mn(1)−O(5)	2.244(8)	Mn(1)−O(10)	1.847(8)
Mn(1)−N(21)	1.957(9)	Mn(1)−N(65)	2.010(8)
Mn(2)−O(1)	1.943(6)	Mn(2)−O(2)	2.229(7)
Mn(2)−O(6)	2.457(7)	Mn(2)−O(30)	1.860(8)
Mn(2)−N(25)	2.008(8)	Mn(2)−N(41)	1.934(8)
Mn(3)−O(1)	1.859(7)	Mn(3)−O(3)	2.098(7)
Mn(3)−O(50)	1.810(8)	Mn(3)−N(45)	2.035(8)
Mn(3)−N(61)	1.958(10)	Mn(1)···Mn(2)	3.338
Mn(1)···Mn(3)	3.269	Mn(2)···Mn(3)	3.227
Bond Angles			
O(1)−Mn(1)−O(4)	90.1(3)	O(1)−Mn(1)−O(5)	88.9(3)
O(1)−Mn(1)−O(10)	178.8(4)	O(1)−Mn(1)−N(21)	89.1(4)
O(1)−Mn(1)−N(65)	88.3(3)	O(4)−Mn(1)−O(5)	176.2(3)
O(4)−Mn(1)−O(10)	89.6(3)	O(4)−Mn(1)−N(21)	93.3(3)
O(4)−Mn(1)−N(65)	82.9(3)	O(5)−Mn(1)−O(10)	91.4(3)
O(5)−Mn(1)−N(21)	90.4(3)	O(5)−Mn(1)−N(65)	93.3(3)
O(10)−Mn(1)−N(21)	89.7(4)	O(10)−Mn(1)−N(65)	92.8(3)
N(21)−Mn(1)−N(65)	175.5(4)	O(1)−Mn(2)−O(2)	90.7(3)
O(1)−Mn(2)−O(6)	89.2(3)	O(1)−Mn(2)−O(30)	175.4(3)
O(1)−Mn(2)−N(25)	90.0(3)	O(1)−Mn(2)−N(41)	87.6(3)
O(2)−Mn(2)−O(6)	176.8(3)	O(2)−Mn(2)−O(30)	92.5(3)
O(2)−Mn(2)−N(25)	91.9(3)	O(2)−Mn(2)−N(41)	93.1(3)
O(6)−Mn(2)−O(30)	87.8(3)	O(6)−Mn(2)−N(25)	84.9(3)
O(6)−Mn(2)−N(41)	90.1(3)	O(30)−Mn(2)−N(25)	93.2(3)
O(30)−Mn(2)−N(41)	88.9(3)	N(25)−Mn(2)−N(41)	174.4(3)
O(1)−Mn(3)−O(3)	90.7(3)	O(1)−Mn(3)−O(50)	177.1(3)
O(1)−Mn(3)−N(45)	88.4(3)	O(1)−Mn(3)−N(61)	88.7(3)
O(3)−Mn(3)−O(50)	88.9(3)	O(3)−Mn(3)−N(45)	101.7(3)
O(3)−Mn(3)−N(61)	116.5(3)	O(50)−Mn(3)−N(45)	94.4(3)
O(50)−Mn(3)−N(61)	88.9(3)	N(45)−Mn(3)−N(61)	141.7(4)
Mn(1)−O(1)−Mn(2)	120.6(4)	Mn(1)−O(1)−Mn(3)	120.9(3)
Mn(2)−O(1)−Mn(3)	116.1(3)		

(primarily) antiferromagnetic interactions between the manganese(III) ions in the trinuclear units.

To further characterize the low-temperature magnetic properties of **2** and **3**, magnetization measurements were carried out at $T = 2$, 4, and 6 K, in fields up to 5 T, see the insets of Figures 3 and 4. At our lowest temperature of 2 K the molar magnetization (M) of complexes **2** and **3** reaches, respectively, a value of 3.1 Nβ and 1.5 Nβ only (per trinuclear complex), even in 5 T. For noninteracting Mn(III) spins such a field/temperature combination would be sufficient to approach the saturation value of $M = 3gS\text{N}\beta = 12\text{N}\beta$ (per trinuclear complex). This is strong evidence for the presence of antiferromagnetic interactions J of the order of a few cm^{-1} in strength, the interaction in **3** being strongest. Furthermore, both compounds show an initially sharper increase of M in low fields, which points to incompletely compensated antiferromagnetic alignment of the spins within the trinuclear units (similar as in the well-known weak ferromagnetic materials). Such an uncompensated component is indeed expected for a triangular spin arrangement on quite general grounds. Only for isotropic Heisenberg interactions between the three spins that are equal in sign (AF) and magnitude, complete compensation is possible, with the spins ordered under angles of 120° to one another, thus resulting in zero net moment for the trinuclear complex. As soon as the interactions become appreciably different, or when anisotropy is introduced, complete compensation will no longer occur. Such will be the situation for our complexes because we cannot expect equal exchange interactions between the three spins on the basis of the molecular structure. Weaker intermolecular interactions between the net moments of the trinuclear units will then become important at low temperature and reduce the total magnetization of the sample (in zero field) to zero. We interpret the initial steeper increase in the magnetization curves seen up to fields of about 1 T in such terms, namely, as the magnetization process whereby these small net moments per cluster become aligned by the applied field. By extrapolating the quasi-linear high-field parts of the magnetization curves to zero field, the size of these net moments δM per cluster can be estimated, giving about 1.2 Nβ and 0.3 Nβ for compounds **2** and **3**, respectively. The fields B_{sat} of order 1 T where this initial process "saturates" give an estimate of the intercluster coupling via the (mean-field) formula: $zJ' \approx g^2\beta^2 B_{sat}/\delta M$, yielding $zJ' \approx 0.1-0.3$ cm^{-1}.

In view of the above, we expect the behavior of the (low-field) susceptibility of **2** and **3** in the low-temperature (<50 K) region to be dominated by the presence of net moments per cluster coupled by weak intermolecular interaction. To obtain quantitative estimates of the intracluster exchange interactions, we therefore restrict our fits of the data to theoretical triangular cluster models, in a first step, to the temperature range above 50 K. In a second step, a molecular field, $B_m = 2zJ'S/g\beta$, representing the intermolecular coupling zJ' is then added, the corrected susceptibility χ' being related to the uncorrected χ by the formula $\chi' = \chi/[1 + \lambda\chi]$ and the molecular field constant given by $\lambda = 2zJ'/g^2\beta^2$ (z being the number of neighboring clusters). In this latter procedure the data are fitted over the whole temperature range covered.

On basis of the nonequivalent exchange paths in the molecular structure, the data above 50 K were thus fitted to the susceptibility calculated from the magnetic energy level spectrum for three spins $S = 2$ coupled by isotropic Heisenberg interactions on the *isosceles* triangle:

$$\hat{H} = -2[J_1(\hat{S}_1\hat{S}_2) + J_1(\hat{S}_1\hat{S}_3) + J_2(\hat{S}_2\hat{S}_3)] \quad (1)$$

where J_1 represents the Mn(III)−Mn(III) exchange interaction parameter of the two exchange paths with similar distances and Mn−O_{oxido}−Mn angle, and J_2 refers to the path characterized by the unique Mn−O_{oxido}−Mn angle. In the case of complex **2**, J_2 is the Mn(2)−Mn(3) interaction (with angle Mn(2)−O(1)−Mn(3) = 116.10°), whereas in **3** it represents the Mn(2)−Mn(3) interaction (with angle Mn(2)−O(1)−Mn(3) = 118.96°). As is well-known,[24] the energy levels for the isosceles triangle of spins S are given by

$$E(S_T, S^*) = -J_1[S_T(S_T+1) - S^*(S^*+1) - S(S+1)] - J_2[S^*(S^*+1) - 2S(S+1)] \quad (2)$$

Here $S^* = S_2 + S_3$ and can take the values $S^* = 2S$, $2S-1$, ..., 0, whereas the total spin $S_T = (S^* + S)$, $(S^* + S - 1)$, ..., $|S^* - S|$. In Figure 5 we plot the so-obtained energy spectrum as $E(S_T, S^*)/|J_1|$ versus the ratio $r = J_2/J_1$. For the lowest levels the corresponding values for the total spin S_T of the trinuclear complex have been indicated. Note that the diagram shown is for antiferromagnetic (negative) values for J_1, for ferromagnetic J_1 the diagram has to be inverted. It

(24) Martin, R. L. *New Pathways in Inorganic Chemistry*; Cambridge University Press: New York, 1968.

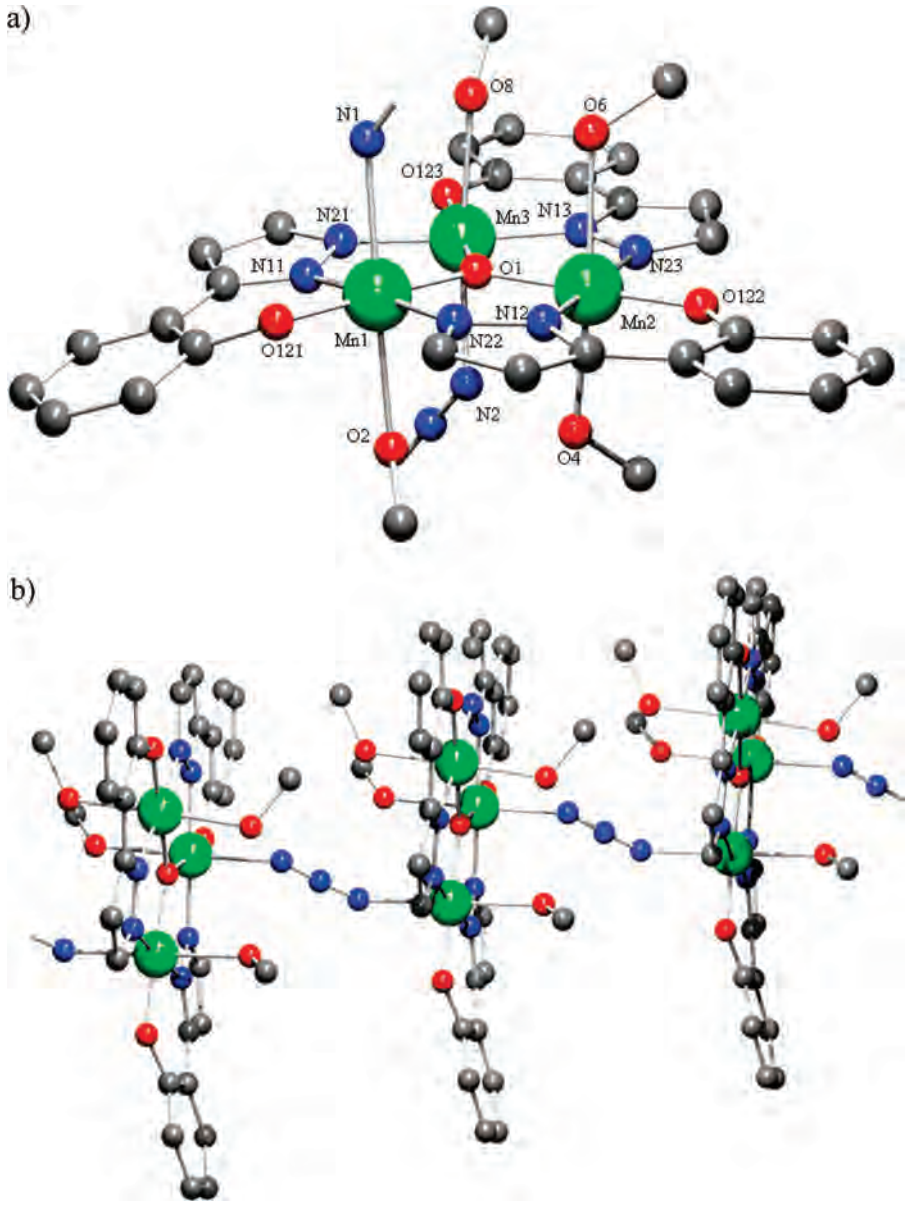

Figure 2. Pluton projection of the complex $[Mn_3(\mu_3\text{-}O)(phpzH)_3(MeOH)_4(N_3)]\cdot MeOH$ **(3)** showing (a) a detailed $Mn_3^{III}O$ unit and (b) the chain of $Mn_3^{III}O$ units bridged by N_3^-. Hydrogen atoms and noncoordinated methanol molecules have been omitted for clarity.

can be seen that only in a small range around the equilateral limit ($J_1/J_2 = 1$) is the ground-state indeed the fully compensated spin state with $S_T = 0$, confirming the qualitative discussion given in the above. For $r < 0.5$ and for all negative values of r, the ground-state is the $E(2,4)$ level, corresponding to net total spin $S_T = 2$ for the trinuclear complex. Furthermore, the total extent of the spectrum is of order 20 to 50 times $|J_1|$, so even for relatively weak exchange constants of a few cm^{-1} it may extend over a few 100 K, explaining why the $\chi_M T$ product is found still varying near room temperature and why the low-T magnetization remains far from saturation even in 5 T (the ferromagnetic state $E(6,4)$ remains far above the ground-state for all r).

For compound **3** the fits of the data above 50 K yielded $J_1 \approx -5.7 \pm 0.3$ cm^{-1}, $J_2 \approx -3.9 \pm 0.2$ cm^{-1}, with $g \approx 2.17 \pm 0.02$. The resulting ratio $r = 0.68$ is close enough to the equilateral limit $r = 1$ for the nonmagnetic $E(0,2)$ level to be still the ground state, see Figure 5. This explains why the $\chi_M T$ product becomes so low for $T = 0$. For the same reason it was found that inclusion of the data over the whole range 2−300 K did not change the values for J_1 and J_2 obtained from the fits. Adding nevertheless in the next step the *inter*molecular interaction zJ', and fitting the data over the whole range, resulted in appreciably better fits, with somewhat different interaction constants $J_1 = -6.6 \pm 0.3$ cm^{-1}, $J_2 = -(4.6 \pm 0.4)$ cm^{-1}, and with $zJ' = +0.7 \pm 0.3$ cm^{-1} and $g = 2.17 \pm 0.02$. The ratio J_2/J_1 thus remains almost the same at $r = 0.70$. We stress that fits to the fully equilateral limit (and obviously without intermolecular interaction) were tried but proved unsuccessful, with appreciable deviation appearing below 40 K.

The best fits of the experimental data for **2** above 50 K gave $J_1 = -(7.2 \pm 0.1)$ cm^{-1}, $J_2 \approx +(7 \pm 2)$ cm^{-1}, and $g = 2.13 \pm 0.04$. Varying the g-value gave systematically higher positive values for J_2 the lower was g, the value for J_1 remaining basically the same. Interestingly, J_2 was always

Table 3. Selected Bonds Lengths [Å] and Angles [°] for the Complex $[Mn_3(\mu_3\text{-}O)(phpzH)_3(MeOH)_4(N_3)]MeOH$ **(3)**

	Bond Lengths		
Mn(1)−O(1)	1.919(2)	Mn(1)−O(2)	2.373(2)
Mn(1)−O(121)	1.884(3)	Mn(1)−N(1)	2.237(2)
Mn(1)−N(11)	1.954(3)	Mn(1)−N(22)	2.008(3)
Mn(2)−O(1)	1.910(3)	Mn(2)−O(4)	2.237(2)
Mn(2)−O(6)	2.341(2)	Mn(2)−O(122)	1.856(3)
Mn(2)−N(12)	1.969(3)	Mn(2)−N(23)	2.027(3)
Mn(3)−O(1)	1.919(2)	Mn(3)−O(8)	2.373(2)
Mn(3)−O(123)	1.864(2)	Mn(3)−N(2)	2.327(3)
Mn(3)−N(13)	1.963(3)	Mn(3)−N(21)	1.991(3)
Mn(1)···Mn(2)	3.329	Mn(1)···Mn(3)	3.326
Mn(2)···Mn(3)	3.299		
	Bond Angles		
O(1)−Mn(1)−O(2)	87.74(10)	O(1)−Mn(1)−O(121)	178.38(10)
O(1)−Mn(1)−N(1)	91.08(13)	O(1)−Mn(1)−N(11)	89.91(11)
O(1)−Mn(1)−N(22)	89.84(11)	O(2)−Mn(1)−O(121)	90.71(10)
O(2)−Mn(1)−N(1)	178.25(14)	O(2)−Mn(1)−N(11)	89.54(10)
O(2)−Mn(1)−N(22)	87.58(10)	O(121)−Mn(1)−N(1)	90.48(13)
O(121)−Mn(1)−N(11)	89.60(12)	O(121)−Mn(1)−N(22)	90.57(12)
N(1)−Mn(1)−N(11)	91.75(13)	N(1)−Mn(1)−N(22)	91.12(13)
N(11)−Mn(1)−N(22)	177.12(11)	O(1)−Mn(2)−O(4)	86.85(10)
O(1)−Mn(2)−O(6)	87.16(10)	O(1)−Mn(2)−O(122)	179.55(10)
O(1)−Mn(2)−N(12)	90.30(12)	O(1)−Mn(2)−N(23)	91.20(11)
O(4)−Mn(2)−O(6)	173.04(10)	O(4)−Mn(2)−O(122)	93.56(10)
O(4)−Mn(2)−N(12)	90.39(10)	O(4)−Mn(2)−N(23)	91.81(10)
O(6)−Mn(2)−O(122)	92.42(10)	O(6)−Mn(2)−N(12)	93.17(10)
O(6)−Mn(2)−N(23)	84.79(9)	O(122)−Mn(2)−N(12)	89.89(12)
O(122)−Mn(2)−N(23)	88.59(12)	N(12)−Mn(2)−N(23)	177.40(11)
O(1)−Mn(3)−O(8)	80.85(9)	O(1)−Mn(3)−O(123)	172.90(11)
O(1)−Mn(3)−N(2)	89.30(12)	O(1)−Mn(3)−N(13)	92.10(11)
O(1)−Mn(3)−N(21)	89.80(12)	O(8)−Mn(3)−O(123)	92.22(10)
O(8)−Mn(3)−N(2)	169.28(12)	O(8)−Mn(3)−N(13)	86.27(10)
O(8)−Mn(3)−N(21)	91.78(11)	O(123)−Mn(3)−N(2)	97.72(12)
O(123)−Mn(3)−N(13)	88.98(11)	O(123)−Mn(3)−N(21)	88.85(12)
Mn(1)−O(1)−Mn(2)	120.79(12)	Mn(2)−O(1)−Mn(3)	118.96(12)
Mn(1)−O(1)−Mn(3)	120.11(14)		

found *ferromagnetic*, except for unreasonably high values of g ($\geq$2.20), where it approached zero. The reason for the wide range of possible J_2 values probably lies in the fact that the $E(2,4)$ level is the ground-state for all negative r values, even up to positive $r = 0.5$, see Figure 5. Furthermore, the nearest excited state $E(3,4)$ runs in parallel at a distance of order 60 K. Indeed, forcing J_2 to be also negative, resulted in lesser fits with very small $J_2 \approx -0.1$ cm^{-1}, whereas J_1 did not change. Adding the *inter*cluster interaction

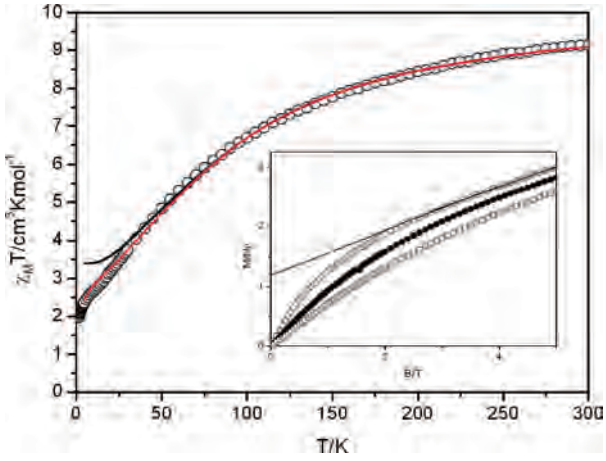

Figure 3. Plot of $\chi_M T$ vs T for **2** in the range 1.8 to 300 K in a 0.1 T field and of the experimental fit (black solid line for isosceles triangle and red solid line considering intermolecular interactions). Inset, field dependence of the magnetization measured at 4 (●), 2 (○) and 6 K (□) and the linear extrapolation of the high-field parts at 2 K.

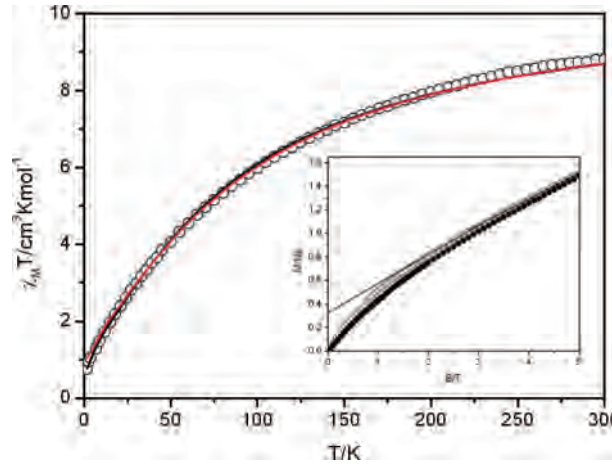

Figure 4. Plot of $\chi_M T$ vs T for **3** in the range 1.8 to 300 K in a 0.1 T field and of the experimental fit (black solid line for isosceles triangle and red solid line considering intermolecular interactions). Inset, field dependence of the magnetization measured at 4 (●) and 2 K (○) and the linear extrapolation of the high-field parts at 2 K.

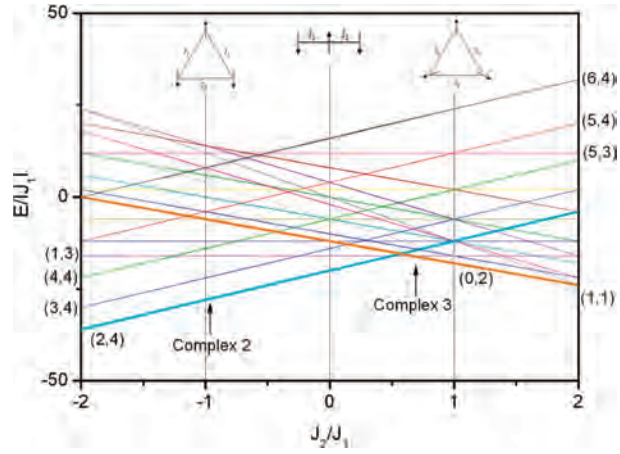

Figure 5. Energy levels for an isosceles triangle with $S_1 = S_2 = S_3 = 2$ calculated for $J_1 < 0$. States are labeled as (S_T, S^*).

zJ' as a molecular field in the next step, we obtained a best fit for $J_1 \approx -(6.8 \pm 0.2)$ cm^{-1}, $J_2 \approx +(7.7 \pm 2.0)$ cm^{-1}, $g = 2.13 \pm 0.3$, and $zJ' \approx -(0.34 \pm 0.03)$ cm^{-1}.

We remark that the values found for zJ' are indeed similar to the rough estimate found above from the initial part of the magnetization curves. They are an order of magnitude larger than the estimated dipolar interaction between cluster moments, indicating the possible presence of superexchange between clusters.

A comment on the g-values exceeding 2.00 resulting from these fits is in order. Although unrealistic for Mn(III), similar values as reported here are often found in the literature (see Table 4) when powder data are fitted with spin-Hamiltonian predictions. The discrepancies probably arise from approximations in the models used, as for instance the neglect of anisotropy as in the present case. Inclusion of the associated crystal field splittings would have made our calculations an order of magnitude more complex. Moreover, we only have powder data available, that is, averages over crystallographic directions, making more detailed fitting less meaningful, also because the anisotropy terms should be relatively small for Mn(III) compounds.

Table 4. Selected Magnetic and Structural Data for Trinuclear Manganese(III) Complexes[a]

complex	J_1/cm^{-1}	J_2/cm^{-1}	g	Mn−O/Å[b]	Mn···Mn/Å[c]	Mn−O−Mn/°[d]	O−Mn_3/Å[e]	ref
				Group I				
$[Mn_3(\mu_3\text{-O})(MeCO_2)_6(py)_3](ClO_4)$	−10.2	−10.2	1.81	1.936	n.r.	120	n.r.	34
$[Mn_3(\mu_3\text{-O})(PrCO_2)_6(py)_3](ClO_4)$	−12.36	−12.36	2.01	1.893	3.272; 3.283; 3.279	121.5; 121.1; 117.3	0.0330	33
$[Mn_3(\mu_3\text{-O})(MeCO_2)_6(3\text{-Mepy})_3](ClO_4)$	−12.87	−12.87	2.22	1.903	3.311; 3.2754; 3.3027	119.99	0.0085	32
$[Mn_3(\mu_3\text{-O})(EtCO_2)_6(3\text{-Mepy})_3](ClO_4)$	−12.31	−12.31	2.12	1.889	3.2662; 3.2691; 3.2800	120 av	0	32
$[Mn_3(\mu_3\text{-O})(Me_3CCO_2)_6(Im)_3](Me_3CCO_2)\cdot 0.5Me_3CCO_2H$	−7.5	−5.2	2.1	A) 1.885; 1.879; 1.890 B) 1.887; 1.880; 1.883	3.260	A) 120.01; 120.18; 119.79 B) 120.24; 119.67; 120.06	A) 0.015 B) 0.019	35
				Group II				
$[Mn_3(\mu_3\text{-O})(MeCO_2)_3(mpko)_3](ClO_4)$	+14.1	+3.8	1.92	1.865; 1.873; 1.865	3.188; 3.203; 3.192	117.08; 117.91; 117.68	0.295	27
$[Mn_3(\mu_3\text{-O})(EtCO_2)_3(mpko)_3](ClO_4)$	+12.1	+1.5	1.92	1.972; 1.874; 2.105	3.260; 3.346; 3.578	115.85; 114.35; 122.65	0.308	26, 28
$[Mn_3(\mu_3\text{-O})(PhCO_2)_3(mpko)_3](ClO_4)$	+18.6	+6.7	1.92	1.880; 1.882; 1.864	3.212; 3.219; 3.200	117.24; 118.47; 117.42	0.286	26
$[Mn_3(\mu_3\text{-O})(MeCO_2)_3(ppko)_3](ClO_4)$	+31.1	+6.7	1.91	1.851; 1.891; 1.872	3.209; 3.190; 3.196	118.03; 115.91; 118.27	0.319	28
				Group III				
$[Mn_3(\mu_3\text{-O})(sao)_3(MeCO_2)(H_2O)(py)_3]$	+4	−10	2.07	n.r.	n.r.	n.r.	0	29
$[Mn_3(\mu_3\text{-O})(sao)_3(PhCO_2)(H_2O)(py)_3]$	+4	−10	1.99	n.r.	n.r.	n.r.	0	29
$[Mn_3(\mu_3\text{-O})(^tBusao)_3(MeOH)_5Cl]$	−0.56	−1.97	1.91	1.895; 1.879; 1.876	3.268, 3.247; 3.265	120.00; 119.73; 119.98	0.059	39
$[Mn_3(\mu_3\text{-O})(^tBusao)_3(Me_3OH)_4(HCO_2)]$	−0.38	−1.37	2.03	1.882; 1.875; 1.879	3.245; 3.261; 3.257	119.45; 120.58; 119.95	0.012	39
$[Mn_3(\mu_3\text{-O})(^tBusao)_3(Me_3OH)_4(N_3)]$	−5.04	−9.51	2.07	1.878; 1.876; 1.885	3.250; 3.259; 3.258	119.90; 120.11; 119.98	0.009	39
$[Mn_3(\mu_3\text{-O})(Me\text{-}sao)_3(MeCO_2)(py)_4]$	−1.06	−2.82	2.03	1.880; 1.899; 1.900	3.239; 3.178; 3.239	117.99; 113.57; 117.89	0.359	40
				Group IV				
$[Mn_3(\mu_3\text{-O})(ppz)_3(MeOH)_3(MeCO_2)]$	−3.01	−3.01	1.88	1.901; 1.909; 1.908	3.297; 3.291; 3.298	119.88; 119.15; 119.98	0.109	11
$[Mn_3(\mu_3\text{-O})(phpzH)_3(MeOH)_3(MeCO_2)]$								this work
$[Mn_3(\mu_3\text{-O})(Meppz)_3(MeOH)_4(MeCO_2)]$	−3.21	−3.21	1.93	1.909; 1.903; 1.915	3.308; 3.297; 3.314	120.42; 119.41; 120.14	0.015	11
$[Mn_3(\mu_3\text{-O})(Meppz)_3(EtOH)_4(MeCO_2)]$	−1.87	−5.61	1.99	1.910; 1.902; 1.911	3.308; 3.276; 3.328	120.43; 118.44; 121.13	0.001	12
$[Mn_3(\mu_3\text{-O})(Brppz)_3(MeOH)_3(N_3)]\cdot 2H_2O$	−3.87	−8.20	2.12	1.922; 1.915; 1.934	3.322; 3.319; 3.329	119.91; 119.17; 119.35	0.139	41
$[Mn_3(\mu_3\text{-O})(Brppz)_3(MeOH)_3(N_3)]$	−4.66	−7.35	2.12	1.898; 1.903; 1.900	3.297; 3.273; 3.299	120.33; 118.75; 120.61	0.062	41
$[Mn_3(\mu_3\text{-O})(phpzMe)_3(Me_3OH)_3(MeCO_2)]$	−6.95	+3.28	2.17	1.900; 1.943; 1.859	3.338; 3.227; 3.269	120.61; 116.10; 120.85	0.172	this work
$[Mn_3(\mu_3\text{-O})(phpzH)_3(MeOH)_4(N_3)]$	−6.77	−3.89	2.2	1.919; 1.910; 1.919	3.329; 3.299; 3.326	120.79; 118.96; 120.11	0.040	this work
				Group V				
$[Mn_3(\mu_3\text{-O})(mpdp)_3(py)_3](ClO_4)$	−8.8 −6.0	−6.2 −10	nr	1.898; 1.888; 1.905	3.275; 3.273; 3.310	119.75; 119.27; 120.98	0.001	44
$[Mn_3(\mu_3\text{-O})(\mu_3\text{-bamen})_3](ClO_4)$	+22.3	+22.3	2.06	1.908; 1.909; 1.898	3.300; 3.303; 3.295	119.67; 120.36; 119.96	0.015	25
$(HNEt_3)_2[Mn_3(\mu_3\text{-O})(bta)_6F_3]$	−5.01	+9.16	2	1.8741; 1.8635; 1.8894	3.226; 3.260; 3.260	119.33; 120.59; 120.06	0.013	45

[a] py = pyridine, 3-Mepy = 3-methylpyridine, Im = imidazole, mpkoH = methyl 2-pyridyl ketone oxime, ppkoH = phenyl 2-pyridyl ketone oxime, H_2sao = salicylaldoxime, ^{t}BusaoH_2 = 3,5-di-*tert*-butylsalicylaldoxime, Me-saoH_2 = methylsalicyloxime, H_2phpzH, H_2ppz = 5(3)-(2-hydroxyphenyl)-pyrazole, H_2Meppz = 3-(5-methyl-2-phenolate)-pyrazole, Brppz = 3-(5-bromo-2-phenolate)pyrazolate, H_2phpzMe = 3(5)-methyl-5(3)-(2-hydroxyphenyl)pyrazole, mpdpH_2 = *m*-phenylenedipropionic acid, H_2bamen = 1,2-bis(biacetylmonoximeimino)ethane, bta = anion of benzotriazole. [b] Mn−μ_3-O^{2-} distance. [c] Mn···Mn distances, Mn(1)···Mn(2); Mn(2)···Mn(3); Mn(1)···Mn(3), respectively. [d] Mn−μ_3-O−Mn angle, Mn(1)−O−Mn(2); Mn(2)−O−Mn(3); Mn(1)−O−Mn(3), respectively. [e] Distance of the μ_3-O^{2-} distance from the Mn_3 plane. A) and B) represent the different units at the unit cell.; av = average; n.r. = not reported.

Notwithstanding such shortcomings, we feel safe in concluding the occurrence of a ferromagnetic interaction J_2 in complex **2**, corresponding to the exchange path with the largest structural distortion of the Mn_3 triangle. For compound **3** the distortion is indeed much smaller and accordingly the J_2 is still antiferromagnetic, although smaller in strength than J_1. The change in sign is of special interest in view of the recent quests for molecular magnetic clusters with high-spin ground states. Indeed, in a number of related $[Mn_3^{III}(\mu_3\text{-O})]^{7+}$ compounds[25–28] even a full ferromagnetic alignment within the molecule, that is, both J_1 and $J_2 > 0$ and thus an $S = 6$ magnetic ground-state at low temperatures, has been reported. Because it is of importance to single out the specific structural features responsible for the ferromagnetic exchange,[29] we shall present in the following section a systematic comparison of the magneto-structural parameters known from the literature for this family of complexes.

Magneto-Structural Correlations. As mentioned, our observation of a ferromagnetic interaction for the Mn(2)−O(1)−Mn(3) bond in complex **2**, which has the strongest distortion of the $[Mn_3(\mu_3\text{-O})]^{7+}$ core, is of special interest in view of the ferromagnetism observed recently in related, high-spin magnetic molecules containing these units, in particular because the great majority of the Mn_3 trinuclear complexes known in the literature show (weak) antiferromagnetism. In this context, the fact that in all these materials the $Mn-O_{oxido}-Mn$ angles are approximately 120° appears to be an important ingredient, since in previous theoretical and experimental studies it has been shown that around this value the net superexchange interaction can be expected to change from antiferromagnetic to ferromagnetic.[30] Whereas the 180° metal−ligand−metal bond is characterized by a relatively strong antiferromagnetic interaction, upon decreasing the bond angle the absolute value decreases and below 120° may become (weakly) ferromagnetic. This prediction appears to be common to the various existing models for superexchange (for a comparative discussion of these models, see ref 31). In all these models, the net interaction J corresponding to the metal−ligand−metal bond arises from the competition of two contributions of opposite sign: $J = J_{AF} + J_F$. Evidently, in the experimental compounds such as the present one, the situation can become much more complex than in the quoted theoretical treatments, for instance, because of the simultaneous presence of several (different) superexchange paths linking the magnetic ions. In addition to the simpler parameters such as the bridging angles between the metal ions, the metal···metal distances, the metal−ligand bond lengths, the overlap of the magnetic orbitals can then depend on the combination of complex structural factors, such as the spatial orientation of Jahn−Teller axes and the dihedral angles between the coordination planes.[15] In a recent paper,[29] Cano et al. have made an attempt by means of density-functional theory (DFT) calculations to evaluate the various structural factors that may be at the origin of the occurrence of ferromagnetic intramolecular interactions in the $[Mn_3^{III}(\mu_3\text{-O})]^{7+}$ cores in some of the Mn_3 triangular complexes. Indeed, because most of the related materials show antiferromagnetism, it is of considerable interest to single out these features in view of the current quests for high-spin Single Molecule Magnets. Although there appears to be an intimate relation with the structural distortion of the $[Mn_3^{III}(\mu_3\text{-O})]^{7+}$ triangle, Cano et al. rightly point out that several other factors may play a role and that a systematic comparison of a series of these compounds would be welcome. To contribute to the discussion of these interesting questions, we have collected in Table 4 relevant magneto-structural data for a large number of related complexes of the family of trinuclear manganese(III). To facilitate the comparison, a subdivision in five groups has been made on basis of structural considerations and/or specific magnetic properties. In Figure 6 a schematic sketch is presented of the $[Mn_3(\mu_3\text{-O})]^{7+}$ core, showing the principal magneto-structural parameters that will be at stake here.

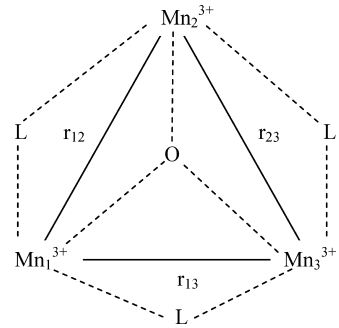

Figure 6. Schematic view of the $[Mn_3(\mu_3\text{-O})]^{7+}$ core with the possible magnetic pathways.

Group I. This first group is formed by the complexes with the general formula $[Mn^{III}_3O(O_2CR)_6(L)_3]^+$ (R = Me, Et, Pr and L = py, 3-Mepy, Im). These complexes have a $[Mn_3(\mu_3\text{-O})]^{7+}$ core, where the oxygen is (almost) within the plane formed by the three manganese(III) ions. Furthermore, the manganese(III) ions form an equilateral triangle, the distances between the manganese(III) ions and the $Mn-O_{oxido}$-Mn angles being basically the same, the latter being close to or equal to 120°, see Table 4. The carboxylates bridge the manganese(III) ions, and the pyridine or the imidazole ligands are at the terminal positions. All of the reported complexes give an antiferromagnetic behavior with a J value around -12 cm^{-1} ($J_1 = J_2 = J$).[32–34] It should be noted that we have included the complex $[Mn_3(\mu_3\text{-O})(O_2CCMe_3)_6(Im)_3]$[35] in this group of complexes with an equilateral triangle, although it was analyzed as isosceles. Indeed, the reported values of J_1 and J_2 are nearly the same, probably because the deviations from 3-fold symmetry are very small.

(25) Sreerama, S. G.; Pal, S. *Inorg. Chem.* **2002**, *41*, 4843–4845.
(26) Stamatatos, T. C.; Foguet-Albiol, D.; Lee, S. C.; Stoumpos, C. C.; Raptopoulou, C. P.; Terzis, A.; Wernsdorfer, W.; Hill, S. O.; Perlepes, S. P.; Christou, G. *J. Am. Chem. Soc.* **2007**, *129*, 9484–9499.
(27) Stamatatos, T. C.; Foguet-Albiol, D.; Stoumpos, C. C.; Raptopoulou, C. P.; Terzis, A.; Wernsdorfer, W.; Perlepes, S. P.; Christou, G. *J. Am. Chem. Soc.* **2005**, *127*, 15380–15381.
(28) Stamatatos, T. C.; Foguet-Albiol, D.; Stoumpos, C. C.; Raptopoulou, C. P.; Terzis, A.; Wernsdorfer, W.; Perlepes, S. P.; Christou, G. *Polyhedron* **2007**, *26*, 2165–2168.
(29) Cano, J.; Cauchy, T.; Ruiz, E.; Milios, C. J.; Stoumpos, C. C.; Stamatatos, T. C.; Perlepes, S. P.; Christou, G.; Brechin, E. K. *J. Chem. Soc., Dalton Trans.* **2008**, 234–240.
(30) Crawford, V. H.; Richardson, H. W.; Wasson, J. R.; Hodgson, D. J.; Hatfield, W. E. *Inorg. Chem.* **1976**, *15*, 2107–2110.

The symmetric triangular coordination in these complexes apparently favors antiferromagnetic interactions between the manganese(III) ions. Furthermore, the ligands terminally coordinated to the metal ions do not appear to play an important role, as the J value does not change significantly when this ligand is varied (other parameters remaining the same). Thus the Mn−O−Mn superexchange path should be the main one responsible for the magnetic interaction, as concluded already by previous authors.[34] Oxido ligands are indeed known to be good bridges for propagating the magnetic superexchange interaction between manganese ions.[36] At the same time, this implies that the structural parameters involved in the $Mn-O_{oxido}-Mn$ bond should be essential for determining the type and strength of the interaction. Because the bond-angle remains almost constant in this group, one expects the strength of the interaction to depend on the Mn−μ_3-O distances. This is indeed observed since with increasing Mn−μ_3-O distance (and thus less overlap of wave functions) the absolute value of J becomes systematically smaller through this series.

Group II. When three carboxylate ligands and the terminal ligands are replaced by the oximato-based bridging ligands mpko and ppko, an important distortion of the $[Mn_3(\mu_3\text{-}O)]^{7+}$ core occurs.[26–28] This structural distortion is reflected in a significant displacement of the central oxido bridge from the plane formed by the three manganese(III) ions (see Table 4), so that the angle $Mn-O_{oxido}-Mn$ becomes appreciably smaller than 120°, the value appropriate for the ideal equilateral triangle. This category of complexes therefore forms an isosceles triangle with two different exchange interactions J_1 and J_2 between the Mn(III) ions that are found to be ferromagnetic, producing a high-spin $S = 6$ ground-state for the molecule. In the recent literature several possible origins for this drastic switch from low-spin to high-spin configuration have been pointed out.[37] First, the distortion from a perfect equilateral triangle will reduce the $Mn_{d\tau}-O_{p\tau}-Mn_{d\tau}$ orbital overlap, thereby weakening the antiferromagnetic contribution to the interaction. Because the superexchange interaction generally is the sum of two competing interactions ($J = J_{AF} + J_F$),[38] the ferromagnetic component along this pathway may then become predominant. Second, it has been pointed out on basis of DFT calculations that the replacement of the carboxylate bridge by the two-atom oximato bridge (nonplanar with the Mn triangle), and the ensuing nonparallel spatial alignment of the Mn(III) Jahn−Teller axes, may have tipped the scales into the direction of ferromagnetism. From such considerations it is evident that as a consequence of the distortion the net value of the exchange will depend on many parameters, and it becomes difficult to distinguish systematic trends, such as a dependence on the Mn−O or the Mn···Mn distances.

Group III. The third group is composed of complexes with salicylaldoxime derivative ligands. Although for the first two members of this group complete crystallographic data are not yet available in the literature, we include them nonetheless, since they were the subject of the mentioned comparative DFT study by Cano et al.[29] The listed parameters have been taken from that publication. These complexes, $[Mn_3(\mu_3\text{-}O)(sao)_3(MeCO_2)(H_2O)(py)_3]$ and $[Mn_3(\mu_3\text{-}O)(sao)_3(PhCO_2)(H_2O)(py)_3]$, as well as $[Mn_3(\mu_3\text{-}O)(^tBusao)_3(MeOH)_5Cl]$,[39] $[Mn_3(\mu_3\text{-}O)(^tBusao)_3(Me_3OH)_4(HCO_2)]$,[39] $[Mn_3(\mu_3\text{-}O)(^tBusao)_3(Me_3OH)_4(N_3)]$,[39] and $[Mn_3(\mu_3\text{-}O)(Me\text{-}sao)_3(py)_4(MeCO_2)]$,[40] all possess an isosceles Mn_3 triangle with different distances between the manganese(III) ions. However, with the exception of the last compound in this group, $[Mn_3(\mu_3\text{-}O)(Me\text{-}sao)_3(py)_4(MeCO_2)]$,[40] in spite of this distortion the central oxygen atom is *(almost) not* displaced from the Mn_3 plane and the $Mn-O_{oxido}-Mn$ angles are *approximately 120°*, similar as for Group I. Because also the Mn−O distances are similar as for Group I, one would expect the antiferromagnetic contribution to the exchange from the $Mn-O_{oxido}-Mn$ paths to be comparable. Furthermore, one may observe that the strengths of the exchange constants found in Groups I and III are roughly comparable, although in Group III one notices a tendency for smaller absolute values and for ferromagnetic interactions. This suggests that the contributions from the carboxylate paths and from the salicylaldoxime paths are comparable, both being weakly antiferromagnetic with a tendency for the latter to be ferromagnetic. In fact, in complexes with salicylaldoxime ligands and higher nuclearity[37] the sign of the exchange has been reported to depend on the Mn−N−O−Mn torsion angle δ. For $\delta < 30.4°$ it was found to be antiferromagnetic, whereas both types of interactions could occur when $\delta \approx 30.4-31.3°$. In all reported trinuclear manganese(III) complexes with salicylaldoxime ligands the torsion angles are below 30.69°, corroborating the presence of antiferromagnetic interactions. In the mentioned DFT study it was found that indeed the oximato torsion angle plays a role because of the orbital countercomplementarity.[29] Interestingly, the compound $[Mn_3(\mu_3\text{-}O)(Me\text{-}sao)_3(py)_4(MeCO_2)]$ can be considered as intermediary between Groups II and III. Although it has a strongly distorted Mn_3 triangle and $Mn-O_{oxido}-Mn$ angles appreciably smaller than 120°, it is still weakly antiferromagnetic. This would imply that the distortion on its own is not a sufficient ingredient for the switch to ferromagnetism.

Group IV. This category is formed by trinuclear complexes with pyrazolates ligands where all of them have the same structural core, $[Mn_3(\mu\text{-}O_3)(phpzR)_3]^+$. The ligands

(31) Vankalkeren, G.; Schmidt, W. W.; Block, R. *Physica B & C* **1979**, *97*, 315–337.

(32) An, J.; Chen, Z. D.; Bian, J. A.; Jin, X. L.; Wang, S. X.; Xu, G. X. *Inorg. Chim. Acta* **1999**, *287*, 82–88.

(33) Li, J.; Yang, S. M.; Zhang, F. X.; Tang, Z. X.; Ma, S. L.; Shi, Q. Z.; Wu, Q. J.; Huang, Z. X. *Inorg. Chim. Acta* **1999**, *294*, 109–113.

(34) Vincent, J. B.; Chang, H. R.; Folting, K.; Huffman, J. C.; Christou, G.; Hendrickson, D. N. *J. Am. Chem. Soc.* **1987**, *109*, 5703–5711.

(35) Baca, S. G.; Stoeckli-Evans, H.; Ambrus, C.; Malinovskii, S. T.; Malaestean, I.; Gerbeleu, N.; Decurtins, S. *Polyhedron* **2006**, *25*, 3617–3627.

(36) Baldwin, M. J.; Stemmler, T. L.; Riggsgelasco, P. J.; Kirk, M. L.; Pennerhahn, J. E.; Pecoraro, V. L. *J. Am. Chem. Soc.* **1994**, *116*, 11349–11356.

(37) Milios, C. J.; Inglis, R.; Vinslava, A.; Bagai, R.; Wernsdorfer, W.; Parsons, S.; Perlepes, S. P.; Christou, G.; Brechin, E. K. *J. Am. Chem. Soc.* **2007**, *129*, 12505–12511.

(38) Hotzelmann, R.; Wieghardt, K.; Florke, U.; Haupt, H. J.; Weatherburn, D. C.; Bonvoisin, J.; Blondin, G.; Girerd, J. J. *J. Am. Chem. Soc.* **1992**, *114*, 1681–1696.

(39) Xu, H.-B.; Wang, B.-W.; Pan, F.; Wang, Z.-M.; Gao, S. *Angew. Chem., Int. Ed.* **2007**, *46*, 7388–7393.

(40) Milios, C. J.; Wood, P. A.; Parsons, S.; Foguet-Albiol, D.; Lampropoulos, C.; Christou, G.; Perlepes, S. P.; Brechin, E. K. *Inorg. Chim. Acta* **2007**, *360*, 3932–3940.

phpzR^{2-} form a plane with the three manganese(III) ions. At the axial position, coordinated solvent molecules are present and other bridging ligands, as acetate and azide, depending on the complex. Two subcategories must be considered depending on whether the $[Mn_3^{III}(\mu_3\text{-O})]^{7+}$ core involves an equilateral or an isosceles triangle.

A model of the equilateral triangle has been considered to evaluate the weak antiferromagnetic exchange interactions for complexes $[Mn_3(\mu_3\text{-O})(Meppz)_3(MeOH)_4(MeCO_2)]$[11] and $[Mn_3(\mu_3\text{-O})(phpzH)_3(MeOH)_3(MeCO_2)]$ **(1)**.[11] Both complexes differ only in the change of the phpzR^{2-} ligand and have Mn−O_{oxido}−Mn angles very close to 120° and nearly equal Mn−O and Mn···Mn distances. However, in the latter complex the central oxygen is appreciably displaced from the Mn_3 plane, implying that the overlap between the magnetic orbitals could be smaller. Nevertheless, the exchange constant are found to be almost equal.

The remaining complexes in Group IV, $[Mn_3(\mu_3\text{-O})(Meppz)_3(EtOH)_4(MeCO_2)]$,[12] $[Mn_3(\mu_3\text{-O})(Brppz)_3(MeOH)_3(N_3)]\cdot 2H_2O$,[41] $[Mn_3(\mu_3\text{-O})(Brppz)_3(MeOH)_3(N_3)]\cdot 2H_2O$,[41] and the complexes **2** and **3**, have been fitted with the isoceles triangle model. Here, there are isolated trinuclear manganese(III) units and 1-D chains comprised of trinuclear manganese(III) units linked by either carboxylates or azides bridges. Once more antiferromagnetic intramolecular interactions are found, except for complex **2** that possesses both ferromagnetic and antiferromagnetic interactions. With the exception of complex **2**, all complexes with pyrazole ligands have a planar $[Mn_3(\mu\text{-}O_3)]^{7+}$ core and angles Mn−O_{oxido}−Mn around 120°, which probably explains the occurrence of antiferromagnetic interactions. Complex **2** shows the most structurally distorted $[Mn_3^{III}(\mu_3\text{-O})]^{7+}$ core, with one of the Mn−O_{oxido}−Mn angles of 116.10° and a deviation of the oxido bridge from the Mn_3 plane of 0.172 Å. In view of the arguments presented for Group II, the smaller Mn−O_{oxido}−Mn angle, corresponding with Mn(2)−O(1)−Mn(3), together with large dihedral angle ($\delta_{pz\text{-}bend}$ = 40.11°) between the least-squares plane of the pyrazole ring and the Mn(2)−N(41)−N(45)−Mn(3) coordination plane, could be held responsible for the observed ferromagnetic interaction along this path. We point out, however, that strong effects of the bridging pyrazole ligands on the type of the magnetic interaction have been reported in other types of systems.[42,43]

Group V. In this group have been included the complexes that could not fit in any of the previous groups. Similar as in the other undistorted complexes, weak antiferromagnetic interactions have been found for $[Mn_3O(mpdp)_3(py)_3](ClO_4)$.[44] By contrast, the complex $[Mn_3(\mu_3\text{-O})(\mu_3\text{-bamen})_3](ClO_4)$[25] in this group makes an interesting comparison, notably with Group II, because a fairly strong ferromagnetic intramolecular interaction is observed, in spite of the fact that the $[Mn_3(\mu_3\text{-O})]^{7+}$ core geometry is *not* distorted. In this material the manganese(III) ions are pentagonal bipyramidally coordinated, instead of having the octahedral geometry as is most commonly observed for trinuclear manganese(III) complexes. In the absence of a distortion, the origin of the ferromagnetic interactions has most probably to be attributed to the superexchange paths along the oximate groups. In the case of $(HNEt_3)_2[Mn_3(\mu_3\text{-O})(bta)_6F_3]$,[45] some difficulties were reported in determining the strength of the interactions and the ground state, suggesting the presence of low-lying excited states, close in energy to the ground state.

Conclusions

The synthesis, crystal structure, and magnetic studies of trinuclear manganese(III)-based complexes have been presented. Mononuclear complexes with the general formula, $[Mn(HphpzR)_2X]$ (R = H, Me, X^- = Br, Cl) have been proven to be excellent starting materials for the synthesis of new manganese(III) clusters with a stable $[Mn_3(\mu_3\text{-O})(phpzR)_3]^+$ core. Methanol molecules are at the terminal positions and bridging ligands such as acetate (Complexes **1** and **2**) or azide (Complex **3**).

Magnetic studies reveal antiferromagnetic intramolecular magnetic interactions for complexes **1** and **3**, whereas complex **2** presents both antiferromagnetic and ferromagnetic interactions between the manganese(III) centers. A magnetostructural study has been performed emphasizing the importance of the structural distortion of the $[Mn_3(\mu\text{-}O_3)]^{7+}$ core on the magnetic properties. Additionally, the coordination geometry of the bridging pyrazole ligands can tune the magnetic exchange interactions. Further work aimed at the synthesis of new complexes exploring the stability of the core $[Mn_3(\mu_3\text{-O})(phpzR)^3]^+$ is in progress.

Acknowledgment. This work was financially supported the EC-RTN "QuEMolNa" (No. MRTN-CT-2003-504880) and the ECNetwork of Excellence "MAGMANet" (No. 515767-2). S.T. acknowledges The Netherlands Organization for Scientific Research (NWO) for a Veni grant. We thank Dr. N. Aliaga-Alcalde for useful discussions.

Supporting Information Available: Hydrogen bonds details for $[Mn_3(\mu_3\text{-O})(phpzMe)_3(MeOH)_3(OAc)]\cdot 1.5MeOH$ **(2)** and for $[Mn_3(\mu_3\text{-O})(phpzH)_3(MeOH)_4(N_3)]MeOH$ **(3)**. Plot of the χ_M and $\chi_M T$ product as a function of temperature for complex **1** (PDF). This material is available free of charge via the Internet at http://pubs.acs.org.

IC8002492

(41) Liu, C. M.; Zhang, D. Q.; Zhu, D. B. *Chem. Commun.* **2008**, 368–370.
(42) Tanase, S.; Koval, I. A.; Bouwman, E.; De Gelder, R.; Reedijk, J. *Inorg. Chem.* **2005**, *44*, 7860–7861.
(43) Ajo, D.; Bencini, A.; Mani, F. *Inorg. Chem.* **1988**, *27*, 2437–2444.
(44) Canada-Vilalta, C.; Huffman, J. C.; Streib, W. E.; Davidson, E. R.; Christou, G. *Polyhedron* **2001**, *20*, 1375–1380.
(45) Jones, L. F.; Rajaraman, G.; Brockman, J.; Murugesu, M.; Sanudo, E. C.; Raftery, J.; Teat, S. J.; Wernsdorfer, W.; Christou, G.; Brechin, E. K.; Collison, D. *Chem.—Eur. J.* **2004**, *10*, 5180–5194.